

# Multi-Wavelength Diagnostics of Pre-Flare Evolution with Aditya-L1: From Chromosphere to Corona

Adithya H.N.<sup>1</sup>\*, Sreejith Padinhatteeri<sup>1</sup>, Soumya roy<sup>1</sup>, Srikanth P<sup>3</sup>, Durhesh Tripathi<sup>2</sup>,

Sankar<sup>3</sup>, Abhilash Sarawade<sup>3</sup>, A N Ramprakash<sup>2</sup>

<sup>1</sup> Manipal Centre for Natural Sciences, Manipal Academy for Higher Education, Manipal, India

<sup>2</sup> Inter University Centre for Astronomy and Astrophysics, Pune, India

<sup>3</sup> U R Rao Satellite Centre, ISRO, Bengaluru, India

Accepted XXX. Received YYY; in original form ZZZ

## ABSTRACT

Exploring the pre-flare phase using Aditya L1 data

**Key words:** keyword1 – keyword2 – keyword3

## 1 INTRODUCTION

Flare is intense, major energy comes from the chromosphere NUV, we can see the chromosphere, suit got high cadence along with hard X-ray and soft X-ray uv observations; kusano and bamba works, Lucia kent and Brandon observed wing enhancement in IRIS (Mg triplet). x-ray observations; Ananth soft X-ray cubesat - abundance change2023,2025, D.Silva-statistical studies 2023, Battaglia2023

pre-flare phase time using spectral signatures from IRIS and EIS

In this Solar Ultraviolet Imaging Telescope (SUIT; D. Tripathi et al. 2017; D. Tripathi et al. 2024; J. Sarkar et al. 2024) on board Aditya-L1 (D. Tripathi et al. 2023, Sarkar et al. (2025),Tripathi et al. (2017),Tripathi et al. (2025),Tripathi et al. (2023))

In this work, we are studying

- (i) What happens in the pre-flare phase of the solar flare (2-hour window).
- (ii) How Chromosphere (Mg II and Ca II H) behaves during the pre-flare phase.
- (iii) Is there a hot X-ray onset in all flares?
- (iv) How Aditya-L1 can be a unique mission for observing Solar flare precursors.

## 2 OBSERVATIONS

In this study, we analyse the pre-flare phase of a solar flare using multiple instruments onboard Aditya-L1, which together provide simultaneous observations of the chromosphere and the corona. The Level-1, Mg II h narrowband Region of Interest (ROI) images ( $\approx 491'' \times 491''$ ) from SUIT/Aditya-L1, with a cadence of approximately 85 s, were used. The data were corrected for scatter and vignetting

For coronal observations, we use data from both SoLEXS (2–22 keV) and HELIOS (CdTe; 10–40 keV), which are high-resolution spectrographs that observe the Sun as a star. We additionally use

Case no.	NOAA no.	Flare class	Flare start time	Flare peak time
Case 4	13738	M1.5	2024-07-10 05:44	2024-07-10 05:59
Case 5	13738	M1.1	2024-07-10 15:25	2024-07-10 15:37
Case 6	13848	X1.8	2024-10-09 01:25	2024-10-09 01:56
Case 7	13878	M1.3	2024-11-01 02:05	2024-11-01 02:16
Case 8	13878	M2.0	2024-11-01 14:18	2024-11-01 14:31
Case 9	13878	M1.0	2024-11-13 00:10	2024-11-13 00:22
Case 10	13878	M1.7	2024-11-13 16:57	2024-11-13 17:08

**Table 1.** Flare cases being studied, the flare class, start time and peak time are based on the GOES flare catalogue

STIX onboard Solar Orbiter for spectral analysis. We restricted our sample to flares of class M and above, located close to disk centre, and with no major (C, M, or X-class) flare occurring within the preceding two hours.

The selected events that satisfy these criteria are listed in Table 1. For comparison of source locations, we additionally incorporate AIA, HMI observations.

For the comparison of source locations, we also use AIA, HMI, and STIX data.

### 2.1 Analysis

To capture the overall behaviour of the active region, we plotted the light curves of the SUIT Mg II h 2803 Å filter. The images were further examined for small-scale brightenings using the image-differencing method. These events were then investigated using complementary coronal observations from SoLEXS and HELIOS. To infer the corresponding spatial locations in the corona, we incorporated observations from AIA and HMI.

\* E-mail: publications@ras.ac.uk (KTS)

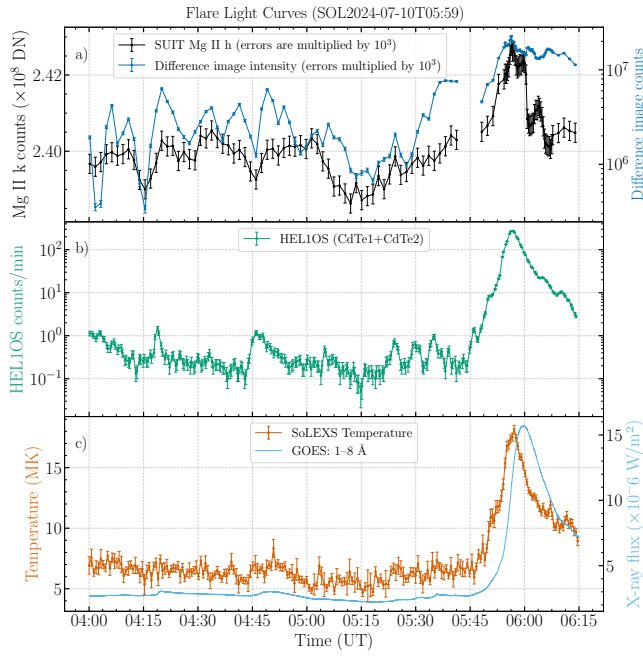


**Figure 1.** a) Total intensity light curve of the Mg II h ROI images (black). The errors of the individual data points are scaled by  $10^3$  for visibility. The light curve of the difference-image intensity above the threshold is shown in cyan, with errors scaled by  $10^4$  for clarity. b) HELIOS light curve (CdTe 1 and CdTe 2, 9–40 keV), binned to 1-minute intervals, c) Temperature derived from SoLEXS(orange) and X-ray flux from the GOES 1–8 Å band (sky blue)

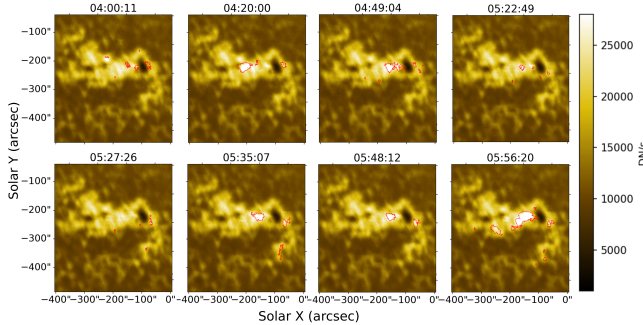


**Figure 2.** Case 4 : SUIT time stamp images of pre-flare enhancements

## 2.2 Flare light curve

All the images are co-aligned using the `mc_coalign` function, publicly available through the `sunkit-image`<sup>1</sup> python package, to remove the satellite drift effect in the image, which will also remove the differential rotation. Further, we selected the common area available in all the frames and plotted the total count of the entire image as a light curve.

## 2.3 Identifying pre-flare enhancements in SUIT

To identify the pre-flare enhancements, we adopted the base-difference method. The base image was constructed using the median

<sup>1</sup> <https://docs.sunpy.org/projects/sunkit-image/en/latest/index.html>

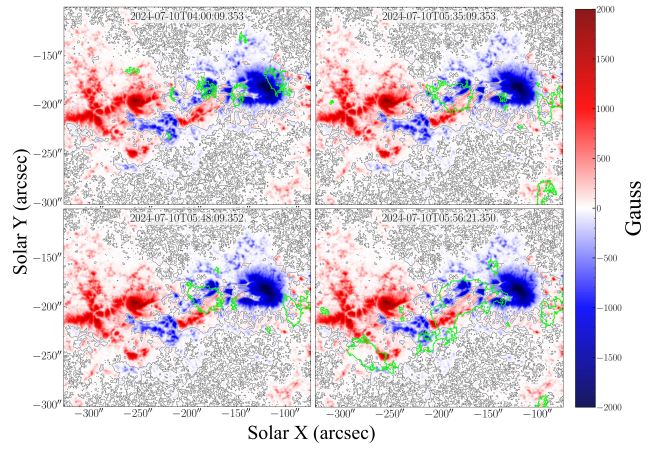


**Figure 3.** Case 4 HMI images, gray colour line represents PIL (0 Gauss value pixels)and green colour contours are SUIT enhancement contours from difference image.

of the first five images in the 2-hour pre-flare image sequence, which also minimises first-frame selection bias. The base-difference images contain quiet-Sun and plage-related fluctuations, as well as intensity fluctuations caused by the contamination pattern. To mitigate these effects, we had to set a threshold to see strong enhancements. Mean and standard deviation of the image were affected by bright events. Therefore, we computed the median and standard deviation( $\hat{\sigma}$ ) from median absolute deviation (MAD) of the difference image, which are less affected by bright events. And we applied the detection threshold given in Eq. 1 to the base-difference image, and contours were drawn around the regions exceeding this threshold.

$$\text{Threshold} = \text{median} + 5\hat{\sigma} \quad (1)$$

$$\hat{\sigma} = k \times \text{MAD} \quad (2)$$

where

$$\tilde{X} = \text{median}(X_i)$$

$$\text{MAD} = \text{median}(|X_i - \tilde{X}|)$$

$$k \approx 1.4826 \text{ (for normal distribution)}$$

Additionally, we imposed a size constraint of 16 pixels (corresponding to a PSF FWHM of  $\approx 8$  pixels). Only features larger than the PSF were retained. The base-difference total intensity within these selected regions was then used to generate the enhancement light curve.

## 2.4 HELIOS light curves

To study simultaneous coronal activity, we consider the HELIOS observations, which cover both thermal and non-thermal parts of the flare (10–40 keV). Multiple count enhancement is observed in the 2-hour pre-flare window, but since it is a sun as a star observation, we cannot say the source is the same active region being observed from SUIT. In most cases, we observe that SUIT enhancement is with by HELIOS enhancements. These enhancements could be small flares; if these enhancements are flares, we expect some non-thermal emission from them. But we have very few counts; we had to integrate over a few minutes to have enough counts to fit the spectra. However, as we integrate over a large time range, we obtain an averaged spectrum, which is essentially a first-order approximation. We compare

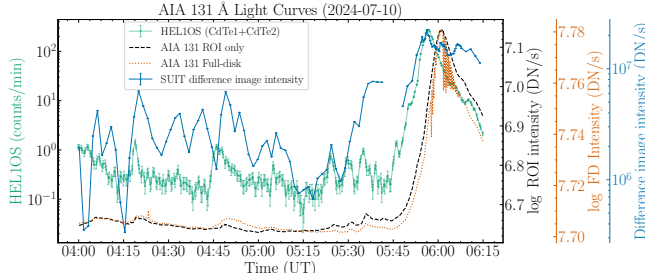


**Figure 4.** AIA 131 Å light curves compared with HELIOS light curve

our estimation with STIX for cases 5 to 10, which is described in section 4.

## 2.5 Temperature from SoLEXS

For the same pre-flare interval, we derived the emission measure and temperature from SoLEXS observations, assuming an isothermal plasma. We had to bin the data for about 2–3 minutes to have enough signal for calculation. SoLEXS temperature follows almost the trend of HELIOS.

## 2.6 Identifying X-ray Source locations on full disc

Both HELIOS and SoLEXS observations come from the Sun as a star observation. We are not sure of the source location of these small enhancements. Using the AIA observation, try to locate the source of these emissions (at least to the active region). AIA 131 Å and AIA 94 Å observe the hot plasma close to the X-ray in the SDO channels.

We plotted the total counts from the full Sun up to  $1.1 R_{\odot}$ , the active region of interest (ROI) observed with SUIT, and the HELIOS counts. The full-disc light curve is expected to mimic observations of the Sun as a star in X-rays. We observe a slight delay between HELIOS and AIA 131 light curves, most likely due to a difference in the energy bands of observation. Each enhancement/event in HELIOS can be connected to one active region (see the figure in the appendix, which includes all light curves). This figure indicates which part of the X-ray light curve should be used to infer information about the active region being observed.

## 2.7 Spectral analysis of pre-flare enhancements

Currently, the HELIOS counts are insufficient to fit the spectra, and with STIX spectra, we are analysing pre-flare enhancements.

## 2.8 Hot onset cases

In most of the flare cases, we observe elevated temperatures during flare onset in SoLEXS. We also notice HELIOS counts increasing during that period. This appears like a hot onset (previously reported, [Hudson et al. \(2021\)](#), [Hudson \(2025\)](#), [Battaglia et al. \(2023\)](#)). We don't have enough counts in HELIOS to conclude that they are of pure thermal nature, but, we have an STIX observation for the last 6 cases; using STIX data, we analyse the pre-flare enhancements and hot onset part by fitting the thermal and non-thermal parts.

## 3 RESULTS

### 3.1 Case 4: M1.5 class flare on July 10 2024

We observe multiple brightenings in the pre-flare window (Fig. B1). All the brightening is occurring on the Polarity Inversion Line (PIL), and some are located close to it (fig 3). Several of the enhancements exhibit corresponding pre-event signatures in HELIOS. To confirm their source locations, we examined the AIA 131 Å images. For three such events, we found a time delay of approximately 90 seconds between the HELIOS signal and the Mg II h response (DCF plot required). The continuous enhancement began to appear at the flaring location after 05:28, which is approximately 31 minutes before the flare's soft X-ray peak time (based on the GOES data). The coronal temperature measured from SoLEXS reaches approximately 6 MK and shows a rapid increase after 05:46, which is about 15 minutes before the soft X-ray peak.

### 3.2 Case 5: M1.1 class flare on July 10 2024

It is another flare from the same active region as above (AR 13878). In this case, we also observe multiple brightenings in the pre-flare window. Four major brightening locations were identified, including flare locations (B1, B2, B3 and B4). All brightenings are on or close to the PIL (Cannot differentiate the exact location due to the PSF size).

After 14:45 onwards continuous brightening is observed, B2 and B3 are constant contributors and B1 is pulsating, note that all three regions are connected (see 171 images in fig ). SoLEXS temperature does not show much variation, it lies between 6–7 MK.

### 3.3 Case 6: X1.8 class flare on October 9 2024

One of the strong flares in our dataset was produced by AR 13848. Minor pre-flare activity was detected in this active region. A small brightening was observed at point 6P1, which may represent a small counterpart of the coronal activity seen in the AIA 171 Å images.

The flare ribbons displayed a flipped ‘S’ morphology, suggesting a sigmoidal flare structure, which is further supported by the XRT soft X-ray observations (attach XRT image).

### 3.4 Case 7: M1.3 class flare on November 1 2024

Similar to the other cases, we also observe pre-flare brightenings in this case. All significant brightenings originate around the flaring location—specifically those for which HELIOS shows enhancements above the error bars. These pre-flare brightenings occur on and close to the polarity inversion line (PIL), whereas the main flare takes place exactly above the PIL.

Using AIA source-localisation techniques, we found that the X-ray peaks correspond to the same region identified in the SUIT observations. STIX spectra for this event show three significant peaks, all exhibiting non-thermal emission, indicating that these correspond to small flare events.

In this case, we do not observe a single continuously enhanced region; instead, the emission is pulsating, consistent with a series of small flares.

### 3.5 Case 8: M2.0 class flare on November 1 2024

Only one enhancement was observed in the pre-flare phase, on the flare location. Pre-flare enhancement and flare are happening slightly

away from PIL. STIX spectral fit suggest that pre-flare enhancement happening at 13:13 is also a small flare. Continuous enhancement started at the flare location and the loop foot point about 30 min earlier than the flare peak.

### 3.6 Case 9: M1.0 class flare on November 13 2024

Only two brightening was observed in pre-flare phase where one among was on the flare location. STIX spectra confirm that small enhancement is the flare. Small continuous enhancement was observed before flare on the flaring location and it stopped just before the flare.

### 3.7 Case 10: M1.7 class flare on November 13 2024

One small enhancement was observed but actual flare was happened another location but still this active region responded, suggesting larger connectivity between active region.

Our pre-flare study suggests that multiple small brightening events are observed in the chromosphere before the flare. This could be due to a small flare or pure thermal events.

Most of the brightening is happening on the PIL, where a flare is going to take place.

All these small events are counter parts of coronal activity .

We observe that some of these events are not started in the same region but are a response to a small event that happened in another region of the sun. This suggests a larger network connecting all active regions.

Summary table

## 4 DISCUSSION

Multiple brightenings on the PIL were observed. It can also be a small flare, since it is solar maximum, not to be confused with just an enhancement and thought of as a precursor.

All these multiple small events could lead to destabilising the larger active region and causing a flare.

especially the event happening just before a flare may be the subject of interest that can tell or that can be the signature of a flare.

Further investigation based on HMI could lead to much more concrete evidence for the flare trigger understanding.

## 5 CONCLUSION

Aditya-L1 can clearly demonstrate the capability of observing pre-flare dynamics in both the chromosphere and the corona by combining both imaging and spectral observations.

Repeating the same procedures during Solar minima could give further confidence in our results.

We need high cadence imaging spectrographs to isolate the source location for better understanding of the solar corona during flares.

## ACKNOWLEDGEMENTS

Acknowledge TMA Pai Scholarship, MCNS, Sunpy, SUIT team, CfA people

## DATA AVAILABILITY

All data are publicly available on the ISSDC-pradan website.

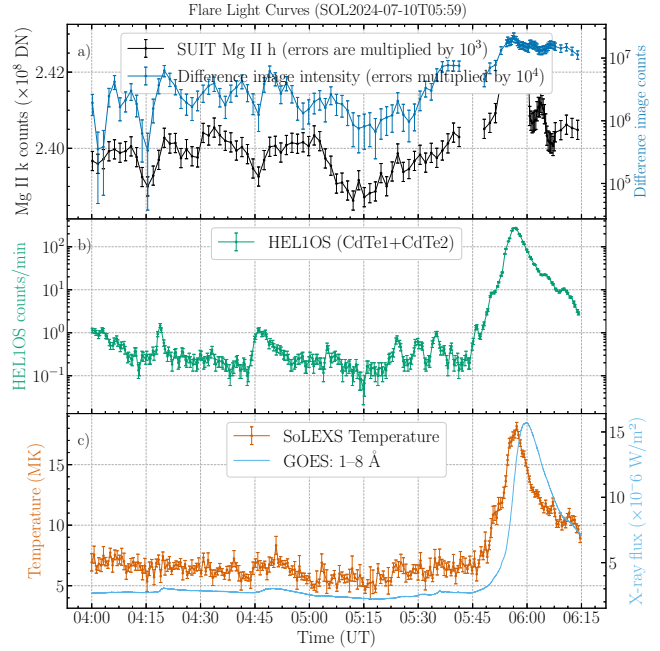


**Figure B1.** Case 4 Light curves

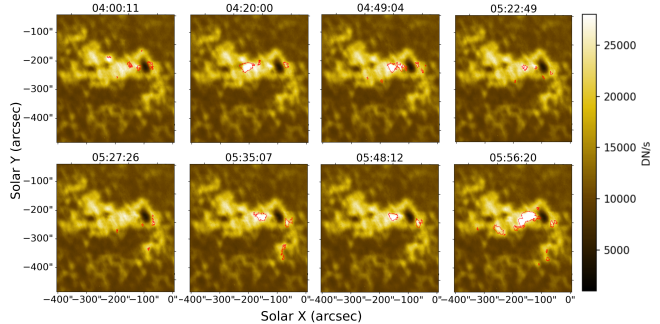


**Figure B2.** Case 4 images

## REFERENCES

- Battaglia A. F., et al., 2023, *Astronomy and Astrophysics*, 679, A139
- Hudson H., 2025, *Solar Physics*, 300, 2
- Hudson H. S., Simões P. J. A., Fletcher L., Hayes L. A., Hannah I. G., 2021, *Monthly Notices of the Royal Astronomical Society*, 501, 1273
- Sarkar J., et al., 2025, Test and Calibration of the Solar Ultraviolet Imaging Telescope (SUIT) on board Aditya-L1, doi:10.48550/arXiv.2503.23476, <https://ui.adsabs.harvard.edu/abs/2025arXiv250323476S>
- Tripathi D., et al., 2017, *Current Science*, 113, 616
- Tripathi D., et al., 2023, in Cauzzi G., Tritschler A., eds, IAU Symposium Vol. 372, The Era of Multi-Messenger Solar Physics. pp 17–27 (arXiv:2212.13046), doi:10.1017/S1743921323001230
- Tripathi D., et al., 2025, *Solar Physics*, 300, 30

Case no.	Pre-flare brightening location	Nature of PFB	Hot onset (Yes/No)	Onset temperature	GOES Flare peak time
Case 4	Flaring location	Continuous	Yes	6-7	5:59
Case 5	Flaring location and closeby	Continuous	No	6-7	15:39
Case 6	Flaring location and closeby	Before flare	No	6-7	01:56
Case 7	Flaring location	Pulasting	No	7-8	02:16

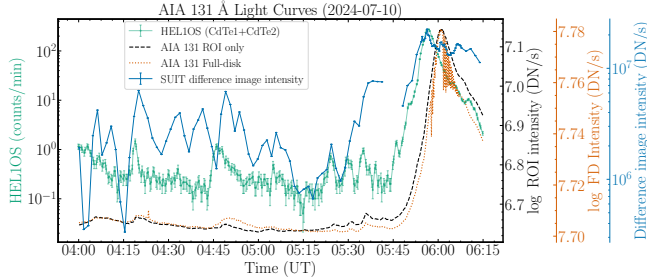


**Figure B3.** Case 4: AIA 131 light curve

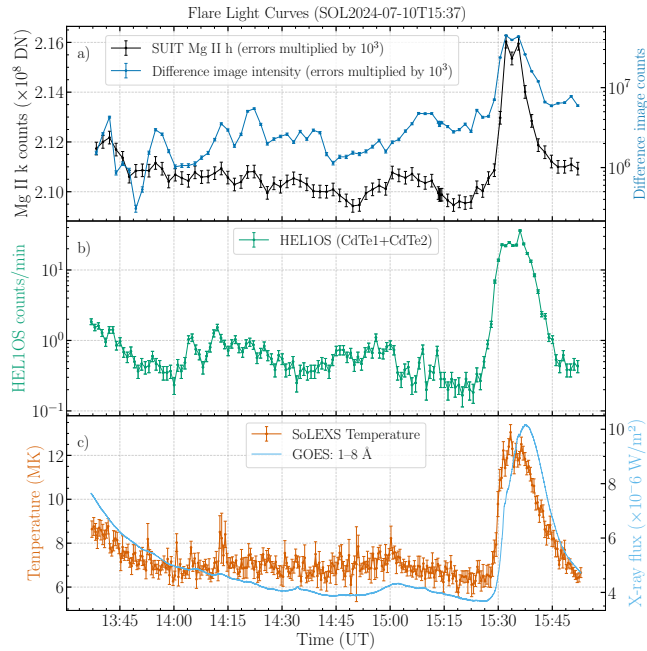


**Figure B4.** Case 5 Light curves

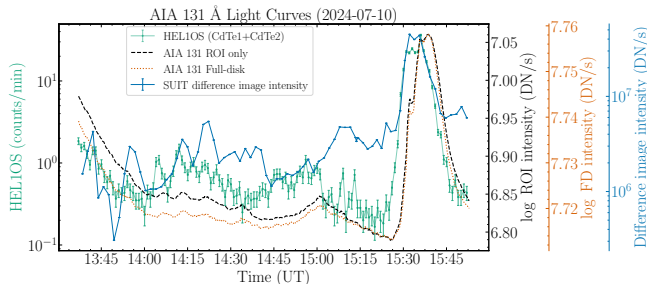


**Figure B5.** Case 5: AIA 131 light curve

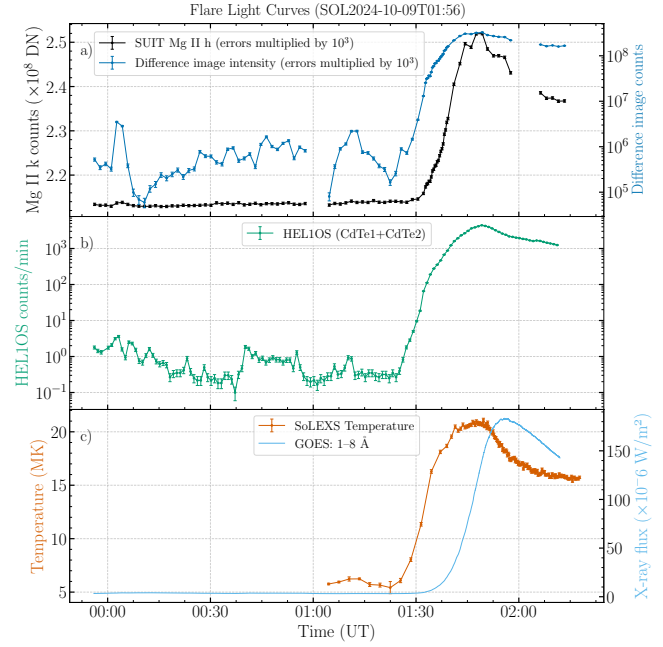


**Figure B6.** Case 6 Light curves

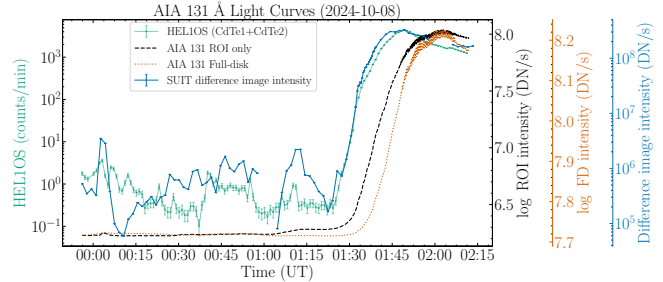


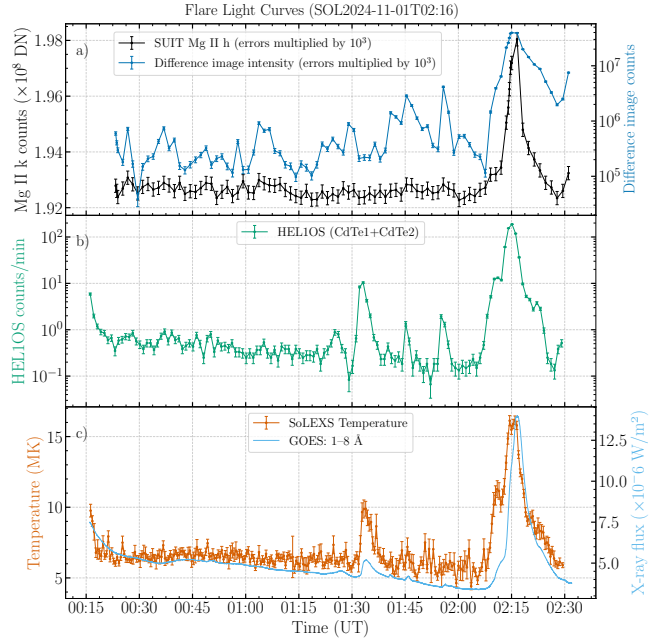
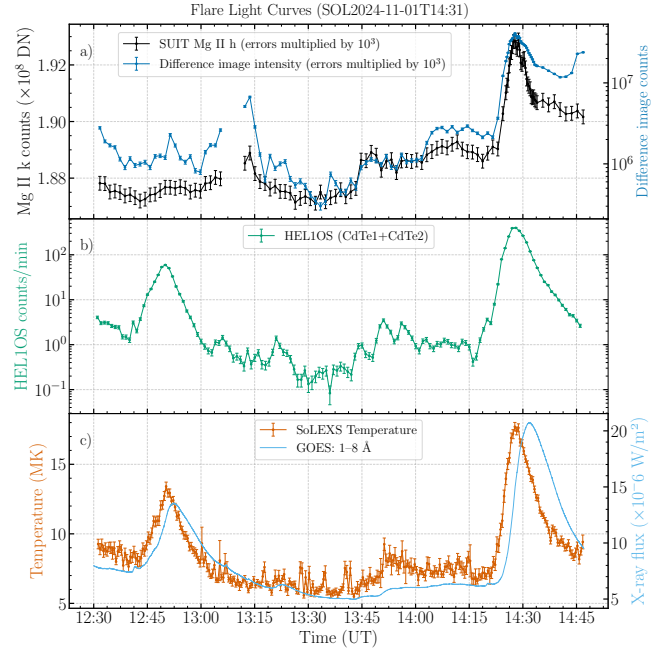
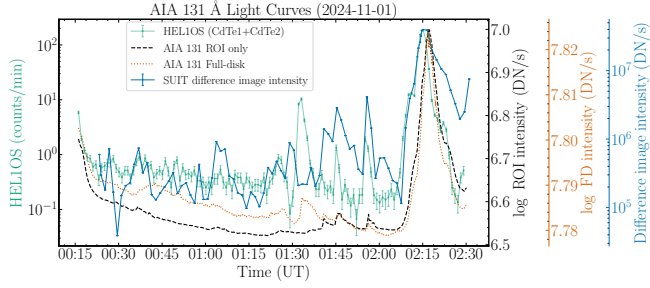
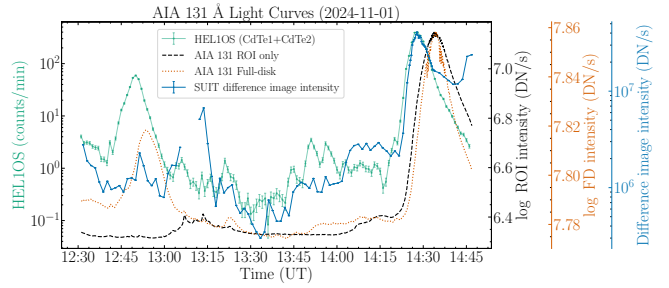
**Figure B7.** Case 6: AIA 131 light curve

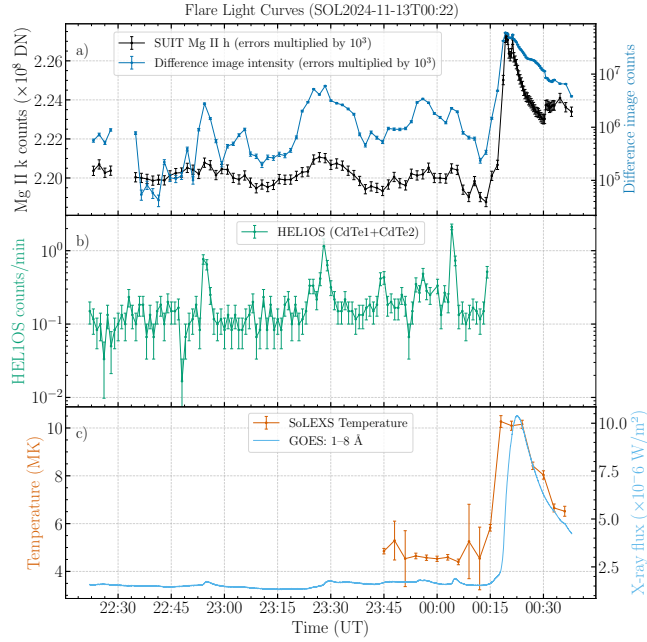
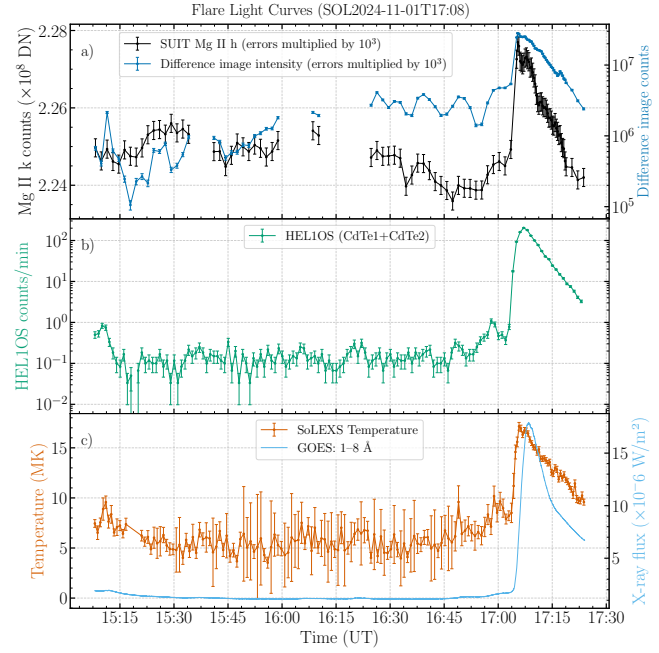
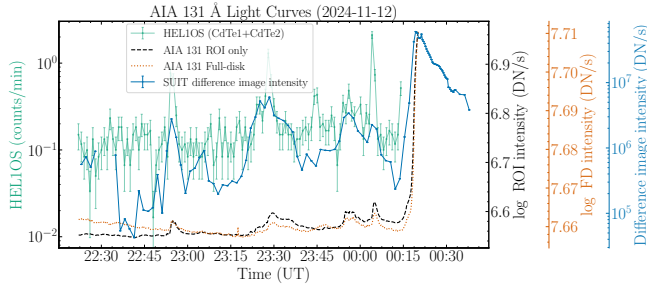
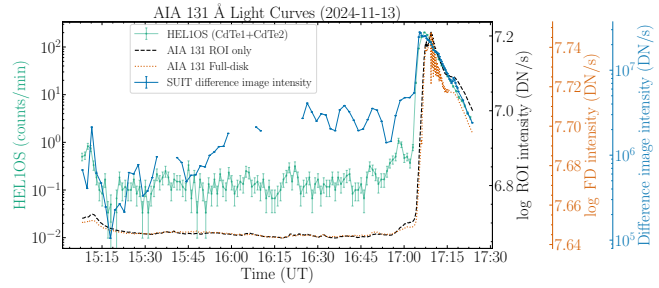
## APPENDIX A: JUSTIFICATION FOR FEW STEPS

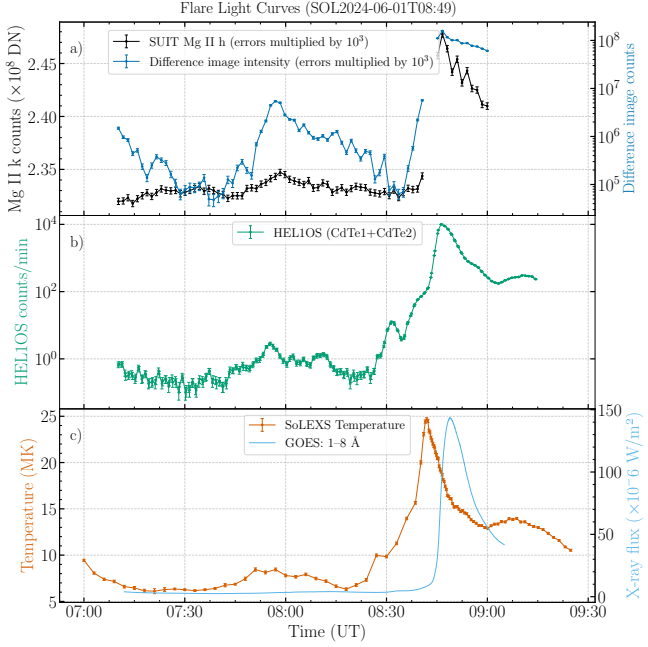
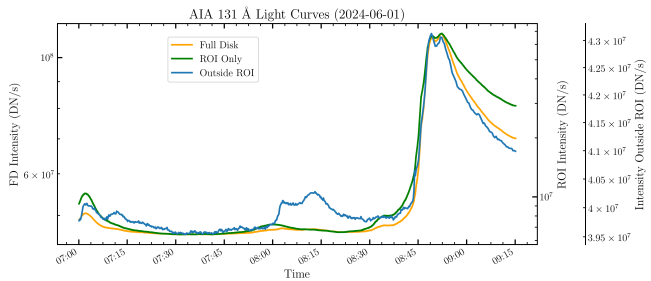
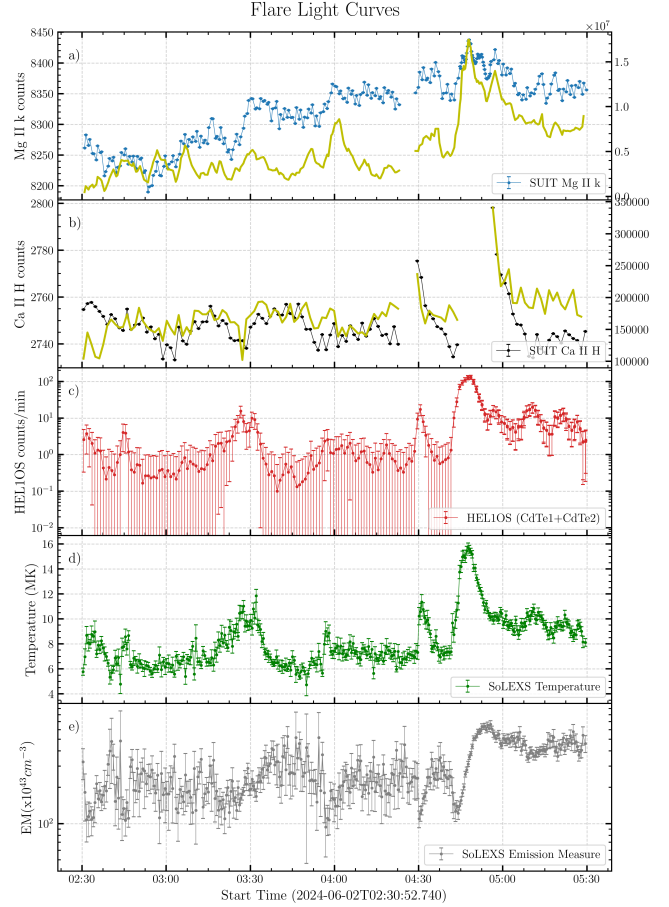
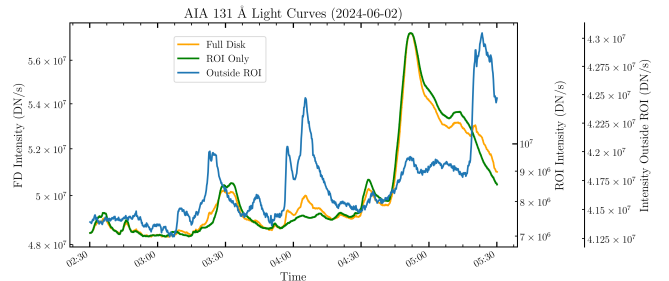
### A1 Difference image threshold

### APPENDIX B: FLARE LIGHT CURVES

This paper has been typeset from a  $\text{\TeX}$ / $\text{\LaTeX}$  file prepared by the author.

**Figure B8.** Case 7 Light curves**Figure B10.** Case 8 Light curves**Figure B9.** Case 7: AIA 131 light curve**Figure B11.** Case 8: AIA 131 light curve

**Figure B12.** Case 9 Light curves**Figure B14.** Case 10 Light curves**Figure B13.** Case 9: AIA 131 light curve**Figure B15.** Case 10: AIA 131 light curve

**Figure B16.** Case 1: June 1st flare**Figure B17.** AIA 131 light curve**Figure B18.** Case 2 light curves**Figure B19.** AIA 131 light curve

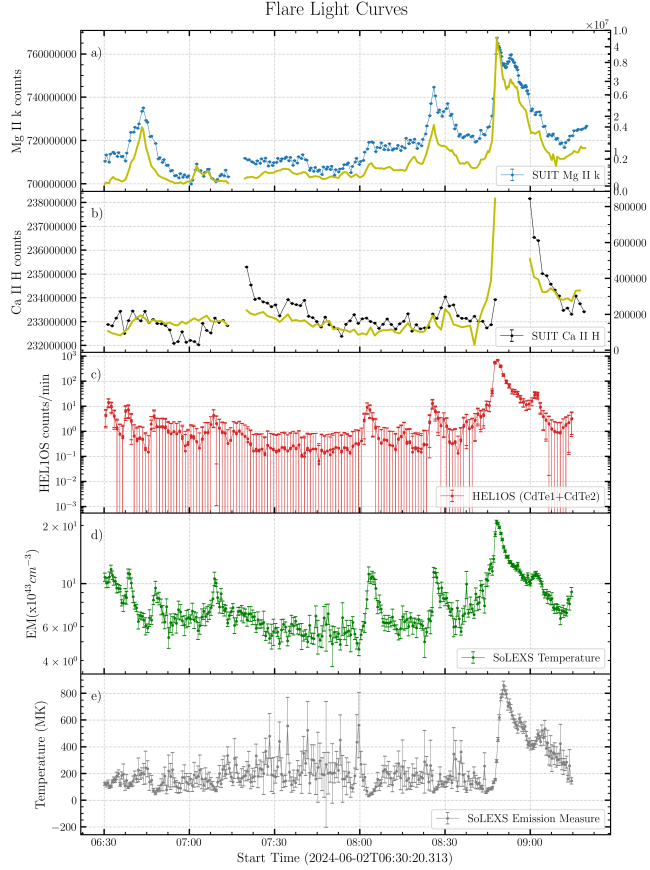


**Figure B20.** Case 3 light curves

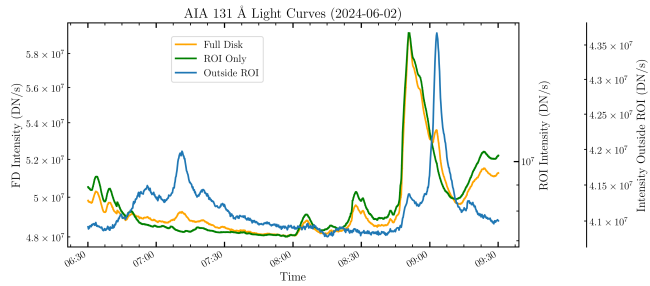


**Figure B21.** AIA 131 light curve